DELIVERABLE REPORT

WP9 JRA4 – Research on Time-resolved ultrafast probes on nanosystems

D9.6

Protocols for temporal characterization of ultrashort FEL pulses

Expected date

M40

NFFA-Europe has received funding from the EU's H2020 framework programme for research and innovation under

nffa.eu

nffa.eu

PROJECT DETAILS

PROJECT ACRONYM	PROJECT TITLE
NFFA-Europe	NANOSCIENCE FOUNDRIES AND FINE ANALYSIS - EUROPE
GRANT AGREEMENT NO:	**FUNDING SCHEME**
654360	RIA - Research and Innovation action
START DATE	
01/09/2015	

WP DETAILS

WORK PACKAGE ID	WORK PACKAGE TITLE
WP9	JRA4 – Research on Time-resolved ultrafast probes on nanosystems

WORK PACKAGE LEADER

Emmanuel Stratakis (FORTH)

DELIVERABLE DETAILS

DELIVERABLE ID	DELIVERABLE TITLE
D9.6	Protocols for temporal characterization of ultrashort FEL pulses

DELIVERABLE DESCRIPTION

Deliverable Description

EXPECTED DATE	ESTIMATED INDICATIVE PERSONMONTHS
31/12/2018	8

AUTHOR

Giovanni De Ninno (UNG)

PERSON RESPONSIBLE FOR THE DELIVERABLE

Emmanuel Stratakis (FORTH)

NATURE

R - Report

DISSEMINATION LEVEL

☒ P - Public
☐ PP - Restricted to other programme participants & EC: (Specify)
☐ RE - Restricted to a group (Specify)
☐ CO - Confidential, only for members of the consortium

REPORT DETAILS

ACTUAL SUBMISSION DATE

21/12/2018

NUMBER OF PAGES

9

FOR MORE INFO PLEASE CONTACT

De Ninno Giovanni (UNG) Tel. +386 5 365 3 521 Email: giovanni.de.ninno@ung.si

Version	Date	Author(s)	Description / Reason for modification	Status
1	16/12/2018	Giovanni De Ninno		Final
				Choose an item.
				Choose an item.
				Choose an item.
				Choose an item.
				Choose an item.

Contents

Executive Summary

The pulse duration, and, more generally, the temporal intensity profile of free-electron laser (FEL) pulses, is of utmost importance for exploring the new perspectives offered by FELs; it is a nontrivial experimental parameter that needs to be characterized. We measured the pulse shape of an extreme ultraviolet externally seeded FEL operating in high-gain harmonic generation mode. Two different methods based on the cross-correlation of the FEL pulses with an external optical laser were used. The two methods, one capable of single-shot performance, may both be implemented as online diagnostics in FEL facilities. The measurements were carried out at the seeded FEL facility FERMI. The FEL temporal pulse characteristics were measured and studied in a range of FEL wavelengths and machine settings, and they were compared to the predictions of a theoretical model. The measurements allowed a direct observation of the pulse lengthening and splitting at saturation, in agreement with the proposed theory.

1. Concept

The advent of FEL sources operating in the vacuum ultraviolet (VUV) or x-ray spectral region has paved the way for time resolution and for the observation of nonlinear and ultrafast processes in the study of the interaction of radiation with matter involving shallow and deep-core electron levels he goal of FELs, in general, is to provide intense and short light pulses with high spectral resolution. Experiments performed at seeded FELs also have the major advantage of the stability of the main pulse parameters such as intensity, duration, time of arrival, and bandwidth. The externally seeded FEL source FERMI, which covers the wavelength range 4 – 100 nm [1,2], is at the cutting edge of this new research field. Along with the energy per pulse, the FEL pulse duration defines the rate of deposited energy on the sample, which drives the onset of nonlinear processes [3] and the modification of absorption [4,5] during sample illumination. In recent years, several indirect [6-9] and direct [10-13] methods have been developed to provide reliable temporal profiles, both on average and on a single-shot basis.

Most of these studies have been performed on self-amplified spontaneous emission (SASE) FEL sources. In contrast, FERMI is an externally seeded FEL source, based on the high-gain harmonic generation scheme (HGHG) [14]. The correlation between FERMI pulse properties and seed pulse properties is well-established. A single-shot spectrotemporal characterization of the seeded FERMI pulses was also carried out in a specific double-pulse configuration by means of the SPIDER technique [15].

We present the first extended study of the FEL pulse temporal properties from a seeded FEL. The study is based on two cross-correlation techniques, aimed at determining the temporal pulse profile of the externally seeded source FERMI in a wide spectral range and for different machine settings. The first cross-correlation between the FEL and an external laser in the gas phase is referred to as method A, and the second method, where the cross-correlation takes place in the solid target, is referred to as method B.

2. Design specification

FERMI is composed of two independent FELs that share the same electron source and photon transport optics. The two sources are identified as FERMI FEL-1 and FERMI FEL-2 (for brevity, FEL-1 and FEL-2, respectively). FEL-1 consists of a single HGHG stage and covers the range 20–100 nm. FEL-2 consists of a double HGHG stage: The first is a shorter replica of FEL-1 whose pulses are used to seed the second stage to produce radiation in the 4–20-nm range. Under optimized conditions, the pulse has a typical energy ranging from a few to hundreds of μJ, with fluctuations that can be as low as 5% (rms, on FEL-1), and a single-mode spectral distribution with Gaussian shape. The full wavelength tunability of FERMI derives from the broad tunability of the seed laser via an optical parametric amplifier (OPA) module and the use of variable gap undulators. The data presented here were collected at the low photon energy FEL-1 and at the first stage of the FEL-2 (indicated as FEL-2.1) sources. FEL-1 delivers photons directly to the end user. FEL-2.1 seeds the second short-wavelength stage of FEL-2, and the pulse properties measured at this intermediate stage provide information on the final pulse properties of FEL-2. Measurements were also done with the FEL operating with the seed generated in two different conditions: as the third harmonic of the Ti: Sapphire laser amplifier (which will be indicated as THG) and as the third harmonic of a wavelength-tunable OPA.

All the optics of the FERMI beam lines (see Fig. 1 and its caption) are reflective, and because of the intrinsic narrow bandwidth of the FEL spectrum, the optical transport system should not affect the FEL pulse length.

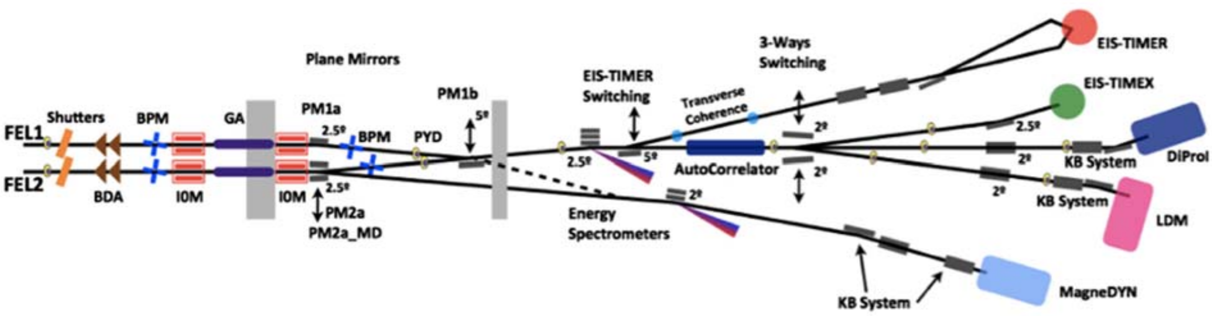

Figure 1: Layout of the FERMI beam transport section. The DiProI and LDM experimental stations share a common photon transport system that includes a beam-defining aperture (BDA), photon beam position monitors (BPM), a gas cell monitoring the FEL fluency (I0M), a gas attenuator (GA), a solid-state photon yield detector (PYD), an energy spectrometer, an autocorrelator, and plane steering mirrors.

2.1 Experimental techniques

Two different experimental setups for the determination of the pulse duration were utilized. One was installed at the low-density matter (LDM) beam line [16] and the other at the diffraction and projection imaging beam line (DiProI) [17]. The experimental techniques adopted on LDM and DiProI are both based on cross-correlation between the FEL pulse and an external laser pulse. This source is the same Ti:Sapphire laser generating the seed for the HGHG process. This solution provides an extremely low jitter between the FEL pulse and the Ti:Sapphire external laser (about 6 fs) and is commonly adopted at FERMI for pump and probe experiments. On the LDM beam line, the pulse duration was measured by monitoring the intensity of sidebands in the photoelectron spectrum of helium as a function of the time delay Δt between the FEL pump pulse and an IR probe pulse. On the DiProI beam line, the cross-correlation was obtained by monitoring the transient transmission change of visible light in a Si_3N_4 membrane induced by the FEL pulse in the so-called tilted-front geometry. The LDM experiment is a direct cross-correlation measurement, but it requires scanning the temporal delay between the FEL and the external laser. The DiProI experiment is more elaborate, but it allows single-shot measurements; in principle, the under-lying method could be used as an online diagnostic in the case of experiments involving transmissive targets.

2.1.1 Two-color photoemission cross-correlation

The physical mechanism behind the FEL-IR cross-correlation signal is the appearance of IR-induced side-bands in a photoelectron spectrum. In our experiment, using a helium gas jet, a single FEL photon promotes one He electron above the ionization potential, giving a photoemission line at energy E0; simultaneous absorption or stimulated emission of one or more IR photons transfers intensity from this main line into satellite peaks, called sidebands. Given the time structure of the IR pulse, the FEL pulse can be deconvolved from the cross-correlation curve. For Gaussian temporal profiles of the two lasers a relation exists between the full width at half maximum (FWHM) of the cross-correlation curve, τ_C, and those of the FEL and IR pulses (τ_{FEL} and τ_{IR}, respectively):

$$\tau_C = \sqrt{\tau_{\mathrm{FEL}}^2 + \frac{\tau_{\mathrm{IR}}^2}{m}}.$$

Photoemission spectra were measured with a custom-made magnetic bottle spectrometer called FERMI-FELCO, akin to the FELCO instrument used at the LCLS [18]. The magnetic bottle is essentially an electron time-of-flight spectrometer (e-TOF) with a static magnetic field shaped to allow collection of electrons over a wide solid angle (4π, for FERMI-FELCO, which, after taking into account the detector efficiency, amounts to an overall efficiency of about 50%). In the case of data acquired from FEL-1, at the working IR intensity of about 3×10^{12} W/cm^2, only two sidebands could be measured (Fig. 2a).

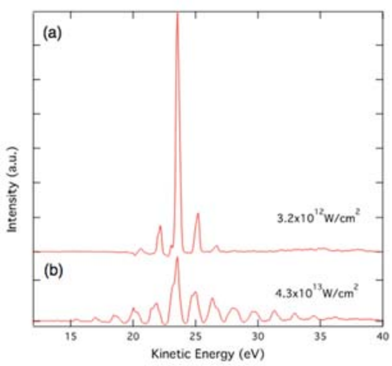

Figure 2: Two-color (FEL at 25.78 nm, IR at 784 nm) photo-electron spectra of atomic He acquired at time delay Δt=0 for IR intensities: (a) about 3.2×10^{12}W/cm^2 (used for the pulse duration on FEL-1) and (b) about 4.3×10^{13} W/cm^2 (maximum intensity available).

The pulse duration values are extracted from SB2. Cross-correlation curves from SB1 and SB2 agree within 10%, which is an indication that saturation effects are not dominant in these conditions. In the case of data acquired from FEL-2.1, the IR intensity was higher, about $1x10^{13}$ W/cm^2, and sidebands up to the fifth order could be measured (Fig. 2b). In this case, the pulse duration values from SB3 and SB4 are consistent within 4%.

2.1.2 High-resolution single-shot solid-state cross-correlation method

The second method is based on ultrafast optical gating. It involves the use of a solid-state target EUV-optical cross-correlation. In such an approach, the FEL pulse is used to excite transient electrons into the conduction band of a dielectric material (Si3N4 for the reported experiment). The wavefront of the FEL is tilted with respect to the target, and the arrival time of each of its portions depends on the spatial positions on the sample. The FEL fluency and the FEL temporal structure are encoded spatially and temporally into the surface of the target. For an accurate determination of the FEL pulse profile, the optical probe pulse must have a known temporal pulse profile. In order to resolve complicated pulse structures, it must be shorter than or comparable to the shortest FEL component. If the probe laser temporal profile is known, the FEL pulse profile can be determined from cross-correlation. Single-shot EUV-optical cross-correlation experiments were carried out at the DiProI end station.

A central element of this experiment was an external compact single-stage NOPA, which was installed on the optical breadboard close to the DiProI experimental end station. Since the available pump probe laser at FERMI is limited to 100 fs, the NOPA is used to generate shorter optical probe pulses in the range of 30 fs in order to improve the temporal resolution of the experiment. The NOPA was tuned to a 630-nm center wavelength generating ~1µJ pulses and compressed in a fused silica prism compressor (Fig.3b). The temporal structure of the NOPA pulses at the target was determined by a SHG autocorrelation measurement and reconstruction of the pulse shape by precisely modeling the pulse spectral phase using known parameters and optics of the setup (Fig.3a).

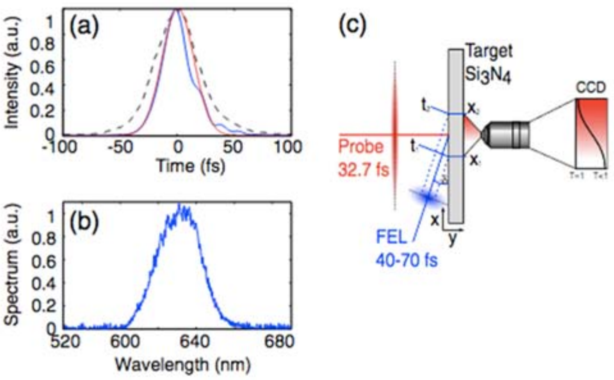

Figure 3: a) Autocorrelation signal (dotted black line) of the noncollinear optical parametric amplifier (NOPA) probe, pumped by the FERMI IR laser (784 nm, 100 fs, 200 µJ). Reconstructed temporal pulse shape from dispersion modeling (blue line) and Gaussian fit of pulse shape (red line). (b) Spectrum of the NOPA signal centered at 630 nm. (c) Schematic of the experimental setup.

3. Results

Measurements with the two methods were carried out in different machine conditions and at different FEL output wavelengths. Different seed pulse durations and different seed pulse generation schemes (OPA or THG) were used for the measurements. As pointed above, the final pulse length is expected to depend on the seed pulse duration and on the FEL harmonic conversion order. The up-shift to a harmonic of order n causes a reduction of the optical pulse duration scaling as $1/\sqrt{n}$ when the FEL is operated far from saturation both in the modulator and/or dispersion section and in the final amplifier. When the output pulse is optimized (maximum bunching at minimum energy modulation the pulse length is expected to scale as about $1/(n)^{1/3}$. The level of saturation can be controlled by varying the intensity of the seed laser.

In Table I, we report a summary of measurements obtained in conditions of almost-single-mode spectra with a pulse energy substantially lower than the maximum available nd measurements in partially saturated conditions.

Table 1: FEL pulse duration data, measured with method (M) A or B, with the harmonic (n) corresponding to the wavelength (λFEL). Seeds at wavelengths (λseed) 261.1 nm and 261.7 nm were generated in THG, while in the other cases, the OPA was used.

M	n	λ_{seed}(nm)	λ_{FEL}(nm)	τ_{seed}(fs)	τ_{FEL}(fs)
A	10	257.8	25.78	140	61.5 ± 3
A	11	261.1	23.74	140	63 ± 4
A	13	261.1	20.08	140	74 ± 3
B	7	261.7	37.38	112.5	52 ± 8
B	10	261.7	26.17	112.5	53 ± 3
B	10	261.7	26.17	157.5	72 ± 6
B	14	261.7	18.69	112.5	42 ± 6
A	7	261.1	37.30	140 ± 2.5	106 ± 2
A	10	257.8	25.78	140 ± 2.5	85 ± 4
A	11	261.1	23.74	140 ± 2.5	95 ± 3

The measurements with method A require the acquisition of data points for different delay times between the FEL and IR pulses. With method B, each measurement is the result of an average over 100 single-shot acquisitions. In Fig. 4, we plot the ratio between the measured FEL pulse length and the seed pulse length, as a function of the harmonic order n for the data in Table I.

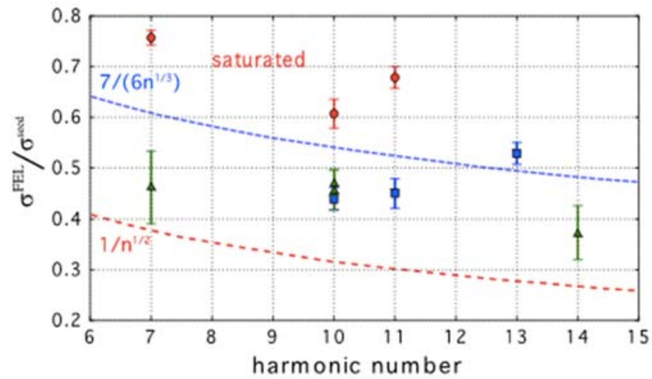

Figure 4: Summary of measurements. Blue squares show method A; green triangles show method B.

The measured pulse durations in blue and green are 15% to 22% lower than the duration estimated in the expected optimized conditions. The data point corresponding to harmonic 13, which shows a slightly larger duration than the $1/(n)^{1/3}$ trend, was measured on FEL-2.1. The anomaly could be associated with a tuning of the FEL, with an increased seed intensity compensating for the lower gain in the amplifier of FEL-2.1 with respect to FEL-1.

4. Conclusions

We have studied the pulse temporal shape and expected behavior of the pulse duration in a seeded FEL operating in the HGHG configuration. We have measured this parameter with two reliable methods: two-color photo-emission cross-correlation and high-resolution single-shot solid-state cross-correlation. The results obtained with the two methods were mutually consistent. Both methods can determine "online" the temporal pulse profile of a FEL, as would be the case for XUV autocorrelation methods. In particular, method B was demonstrated in a single-shot mode. Pulse characteristics, such as the pulse splitting at saturation, were uniquely determined.

References

[1] E. Allaria et al., Nat. Photonics 6, 699 (2012)

[2] E. Allaria et al., Nat. Photonics 7, 913 (2013)

[3] N. Berrah et al., J. Mod. Opt. 57, 1015 (2010)

[4] L. Young et al., Nature 466, 56 (2010)

[5] B. Nagler et al., Nat. Phys. 5, 693 (2009)

[6] C. Behrens et al., Phys. Rev. ST Accel. Beams 15, 030707 (2012)

[7] C. Behrens et al., Nat. Commun. 5, 3762 (2014)

[8] A. A.Lutman et al., Phys. Rev. ST Accel. Beams 15, 030705 (2012)

[9] Y. Inubushi, Phys. Rev. Lett. 109, 144801 (2012)

[10] R. Mitzner at al., Phys. Rev. A 80, 025402 (2009)

[11] R. Riedel et al., Nat. Commun. 4, 1731 (2013)

[12] U. Frühling et al., Nat. Photonics 3, 523 (2009)

[13] I. Grgura et al., Nat.Photonics 6, 852 (2012)

[14] L. H. Yu, Phys. Rev. A 44, 5178 (1991)

[15] G. De Ninno et al., Nat. Commun. 6, 8075 (2015)

[16] C. Svetina et al., J. Synchrotron Radiat. 22, 538 (2015)

[17] F. Capotondi et al., Rev. Sci. Instrum. 84, 051301 (2013)

[18] L. J. Frasinski et al., Phys. Rev. Lett. 111 , 073002 (2013).